Eur. Phys. J. AP **7**, 19–24 (1999)

THE EUROPEAN PHYSICAL JOURNAL APPLIED PHYSICS

Magneto-optical properties of metal-dielectric composites with a periodic microstructure

Y.M. Strelniker[a] and D.J. Bergman

School of Physics and Astronomy, Raymond and Beverly Sackler Faculty of Exact Sciences, Tel Aviv University, Tel Aviv 69978, Israel

Received: 2 December 1998 / Revised: 19 March 1999 / Accepted: 21 April 1999

Abstract. The AC magneto-electric properties (including Faraday rotation, etc.) of a metal-dielectric composite are considered in the quasi-static regime. Resonances appear at modified values of the surface plasmon and cyclotron frequencies, which depend on the applied magnetic field as well as on the microstructure. When the microstructure is periodic and has more than one characteristic length scale, the electric permittivity can exhibit a strong dependence on both the magnitude and the direction of the applied DC magnetic field in the vicinity of one of those resonances. The possibility of observing this effect in a suitably fabricated composite film is discussed.

PACS. 78.20.Ls Magnetooptical effects – 77.84.Lf Composite materials – 77.22.Ch Permittivity (dielectric function)

1 Introduction

Recent technical advances permit the fabrication of made-to-order composite thin semiconducting films with a microstructure that is quite complicated. Such structured films are, in some sense, a new form of matter, and the study of their physical properties is being pursued by a rapidly growing number of research groups. Very recently, the phenomenon of induced anisotropic DC magneto-transport in a composite conductor with a periodic microstructure was first predicted and studied theoretically and numerically [1–4], and then verified experimentally [5]. Here we discuss the possibility of observing analogous behavior in the AC electric permittivity of a metal-dielectric composite with a periodic microstructure in the presence of a strong static magnetic field $\mathbf{B}$.

2 Theory

We consider a two-component metal-dielectric composite medium made of two uniform materials. In accordance with the theory developed for such systems [1,2] we assume that the host medium, with a single or multiple inclusions, occupies the entire volume in between the infinitely conducting plates of a large capacitor, the parallel plates of which are perpendicular to the α-axis, along which the static uniform electric field $E_{0,\alpha} = \nabla r_\alpha = e_\alpha$ is applied. The local electrical potential $\phi^{(\alpha)}(\mathbf{r})$ is usually taken to be determined as the solution of a boundary value problem, based upon a partial differential equation that follows from the requirement that the divergence of the electric displacement $\mathbf{D} = \hat{\boldsymbol{\varepsilon}} \cdot \nabla\phi$ must vanish. This can be written in the following form:

$$\nabla \cdot \hat{\boldsymbol{\varepsilon}} \cdot \nabla\phi^{(\alpha)} = \nabla \cdot \theta_{\rm inc}\delta\hat{\boldsymbol{\varepsilon}} \cdot \nabla\phi^{(\alpha)}, \quad \text{in the entire system volume,} \tag{1}$$

$$\phi^{(\alpha)} = r_\alpha, \quad \text{on the system surface,} \tag{2}$$

$$\delta\hat{\boldsymbol{\varepsilon}} \equiv \hat{\boldsymbol{\varepsilon}} - \hat{\boldsymbol{\varepsilon}}_{\rm inc}. \tag{3}$$

Here r_α is the α-component of $\mathbf{r}$, $\hat{\boldsymbol{\varepsilon}}_{\rm inc}$ and $\hat{\boldsymbol{\varepsilon}}$ are the electrical permittivity tensors of the inclusions and the host respectively, $\theta_{\rm inc}$ is the characteristic or indicator function describing the locations and the shapes of the inclusions (it is equal to 1 inside the inclusions and to 0 in the host medium). The boundary value problem (1, 2) can be transformed to the following integro-differential equation:

$$\phi^{(\alpha)}(\mathbf{r}) = r_\alpha + \hat{\Gamma}\phi^{(\alpha)}, \tag{4}$$

$$\hat{\Gamma}\phi \equiv \int {\rm d}V' \theta_{\rm inc}(\mathbf{r}')\nabla' G(\mathbf{r},\mathbf{r}'|\hat{\boldsymbol{\varepsilon}}) \cdot \delta\hat{\boldsymbol{\varepsilon}} \cdot \nabla'\phi(\mathbf{r}'), \tag{5}$$

where G is the Green function of the left-hand-side of equation (1) (the symmetric part of $\hat{\boldsymbol{\varepsilon}}$ is assumed to be diagonal):

$$G(\mathbf{r},\mathbf{r}'|\hat{\boldsymbol{\varepsilon}}) = \frac{1}{4\pi\left(\varepsilon_{xx}\varepsilon_{yy}\varepsilon_{zz}\right)^{1/2}} \times \left[\frac{(x-x')^2}{\varepsilon_{xx}} + \frac{(y-y')^2}{\varepsilon_{yy}} + \frac{(z-z')^2}{\varepsilon_{zz}}\right]^{-1/2}. \tag{6}$$

[a] e-mail: strel@post.tau.ac.il

2.1 Multiple periodically arranged inclusions

Further treatment depends upon whether we consider a single or multiple inclusions. In the case of periodically arranged inclusions, we can subtract the linear part $r^{(\alpha)}$ from the electrical potential $\phi^{(\alpha)}$ and expand the remaining periodic part $\psi^{(\alpha)} = \phi^{(\alpha)} - r^{(\alpha)}$, as well as $\theta_{\rm inc}$, in Fourier series. Solving the system of linear equations obtained in this way from (4), we find the Fourier coefficients of $\psi(\mathbf{r})$

$$\psi_{\mathbf{g}}^{(\alpha)} = \frac{1}{V_a}\int_{V_a}\psi(\mathbf{r})\mathrm{e}^{-\mathrm{i}\mathbf{g}\cdot\mathbf{r}}\mathrm{d}V. \tag{7}$$

Here $\mathbf{g}$ is a vector of the appropriate reciprocal lattice and V_a is the volume of a unit cell. This can then be used to calculate the bulk effective macroscopic electrical permittivity tensor $\hat{\boldsymbol{\varepsilon}}^{(\mathrm{e})}$, using the procedure described in references [1,2].

2.2 Single inclusion

Equation (4) can be solved also for the single ellipsoidal inclusion problem. From equations (4–6) it follows that, when an external static or quasi-static electric field $\mathbf{E}_0$ is applied, a dipole moment is induced which is responsible for the depolarization effect, *i.e.*, the internal field $\mathbf{E}$ differs from $\mathbf{E}_0$. Actually, if we differentiate equation (4) by $\mathbf{r}$ and take into account equation (6) written for an isotropic host $\varepsilon_{xx} = \varepsilon_{yy} = \varepsilon_{zz} = \varepsilon$ (the case of an anisotropic host is discussed in Ref. [6]) we get

$$E_\alpha(\mathbf{r}) = E_{0\alpha} + \frac{1}{\varepsilon}\sum_{\beta\gamma}\int_{V_{\rm inc}}\mathrm{d}\mathbf{r}'\frac{\partial}{\partial r_\alpha}\frac{\partial}{\partial r'_\beta}\frac{1}{4\pi|\mathbf{r}-\mathbf{r}'|}\delta\varepsilon_{\beta\gamma}E_\gamma(\mathbf{r}'), \tag{8}$$

where the integration volume $V_{\rm inc}$ is the volume of the inclusion. We now recall the fact that, if both $\hat{\boldsymbol{\varepsilon}}_{\rm inc}$ and $\hat{\boldsymbol{\varepsilon}}$ are scalar tensors, and if $\mathbf{E}_0$ lies along a principal axis α of an isolated ellipsoidal inclusion, then the electric field inside that inclusion is uniform and points in the same direction, and its magnitude is given by $E_{0\alpha}\varepsilon/\left[\varepsilon_{\rm inc}n_\alpha + \varepsilon(1-n_\alpha)\right]$, where n_α is the appropriate depolarization factor (see Ref. [8]). Comparing this expression with equation (8) it is easy to show that the electric field is uniform inside the inclusions even though $\hat{\boldsymbol{\varepsilon}}_{\rm inc}$ is a non-scalar tensor due to the presence of a magnetic field. Thus, $\mathbf{E}(\mathbf{r}')$ can be factored out from the integral sign in equation (8) and its values there satisfy (see also Refs. [6–10])

$$E_\alpha = E_{0,\alpha} + \frac{n_\alpha}{\varepsilon}\sum_\beta\delta\varepsilon_{\alpha\beta}E_\beta, \tag{9}$$

where the coordinate axes are chosen to lie along the principal axes of the inclusion and

$$n_\alpha = -\int_{V_{\rm inc}}\mathrm{d}\mathbf{r}'\frac{\partial^2}{\partial r_\alpha^2}\frac{1}{4\pi|\mathbf{r}-\mathbf{r}'|}\quad\text{for}\quad\mathbf{r}\in V_{\rm inc}, \tag{10}$$

is the depolarization factor (which depends only on the precise shape of the inclusion) along the α-axis.

For the sake of definiteness, let us assume that the host is described by a scalar local electrical permittivity $\hat{\boldsymbol{\varepsilon}} = \varepsilon\hat{\mathbf{I}}$ (where $\hat{\mathbf{I}}$ is the unit tensor), while the metallic inclusions are described by an AC permittivity tensor, which, in the presence of a static magnetic field $\mathbf{B} \parallel z$, can be written in quasi-static approximation as

$$\hat{\boldsymbol{\varepsilon}}_{\rm inc} = \varepsilon_{\rm inc}\hat{\mathbf{I}} + \mathrm{i}\frac{4\pi}{\omega}\hat{\boldsymbol{\sigma}} \tag{11}$$

$$= \varepsilon_{\rm inc}\hat{\mathbf{I}} + \mathrm{i}\omega_{\rm p}^2\frac{\tau}{\omega} \times\begin{pmatrix} \frac{1-\mathrm{i}\omega\tau}{(1-\mathrm{i}\omega\tau)^2+H^2} & \frac{-H}{(1-\mathrm{i}\omega\tau)^2+H^2} & 0\\ \frac{H}{(1-\mathrm{i}\omega\tau)^2+H^2} & \frac{1-\mathrm{i}\omega\tau}{(1-\mathrm{i}\omega\tau)^2+H^2} & 0\\ 0 & 0 & \frac{1}{1-\mathrm{i}\omega\tau}\end{pmatrix}. \tag{12}$$

Here $\varepsilon_{\rm inc}$ is the scalar dielectric constant, and we used the free-electron Drude approximation for the conductivity tensor $\hat{\boldsymbol{\sigma}}$. We also used H to denote the Hall-to-Ohmic resistivity ratio $H \equiv \rho_{\rm H}/\rho = \sigma_{xy}/\sigma_{xx} = \mu|\mathbf{B}| = \omega_{\rm c}\tau$, where $\omega_{\rm c} = eB/mc$ is the cyclotron frequency, τ is the conductivity relaxation time, $\omega_{\rm p} = \left(4\pi e^2N_0/m\right)^{1/2}$ is the plasma frequency, N_0 is the charge carrier concentration, and μ is the Hall mobility.

Solving the system of linear equations (9), we obtain the following expression for the uniform electric field inside the inclusion, for the case where $\mathbf{B} \parallel z$

$$\mathbf{E} = \hat{\boldsymbol{\gamma}}\cdot\mathbf{E}_0, \tag{13}$$

$$\hat{\boldsymbol{\gamma}} = \begin{pmatrix} \frac{1}{D}\left(1-n_y\frac{\delta\varepsilon_{yy}}{\varepsilon_{yy}}\right) & \frac{1}{D}n_x\frac{\delta\varepsilon_{xy}}{\varepsilon_{xx}} & 0\\ \frac{1}{D}n_y\frac{\delta\varepsilon_{yx}}{\varepsilon_{yy}} & \frac{1}{D}\left(1-n_x\frac{\delta\varepsilon_{xx}}{\varepsilon_{xx}}\right) & 0\\ 0 & 0 & \frac{1}{1-n_z\frac{\delta\varepsilon_{zz}}{\varepsilon_{zz}}}\end{pmatrix}, \tag{14}$$

$$D = \left(1-n_x\frac{\delta\varepsilon_{xx}}{\varepsilon_{xx}}\right)\left(1-n_y\frac{\delta\varepsilon_{yy}}{\varepsilon_{yy}}\right) - n_xn_y\frac{\delta\varepsilon_{xy}}{\varepsilon_{xx}}\frac{\delta\varepsilon_{yx}}{\varepsilon_{yy}}\,. \tag{15}$$

The bulk effective electric permittivity tensor is defined by (the angular brackets denote a volume average)

$$\hat{\boldsymbol{\varepsilon}}^{(\mathrm{e})}\cdot\langle\mathbf{E}(\mathbf{r})\rangle \equiv \langle\hat{\boldsymbol{\varepsilon}}(\mathbf{r})\cdot\mathbf{E}(\mathbf{r})\rangle. \tag{16}$$

For a dilute system it immediately follows that

$$\hat{\boldsymbol{\varepsilon}}^{(\mathrm{e})} = \hat{\boldsymbol{\varepsilon}} - p_{\rm inc}\delta\hat{\boldsymbol{\varepsilon}}\cdot\hat{\boldsymbol{\gamma}}, \tag{17}$$

where $p_{\rm inc} = V_{\rm inc}/V$ is the volume fraction of the inclusions.

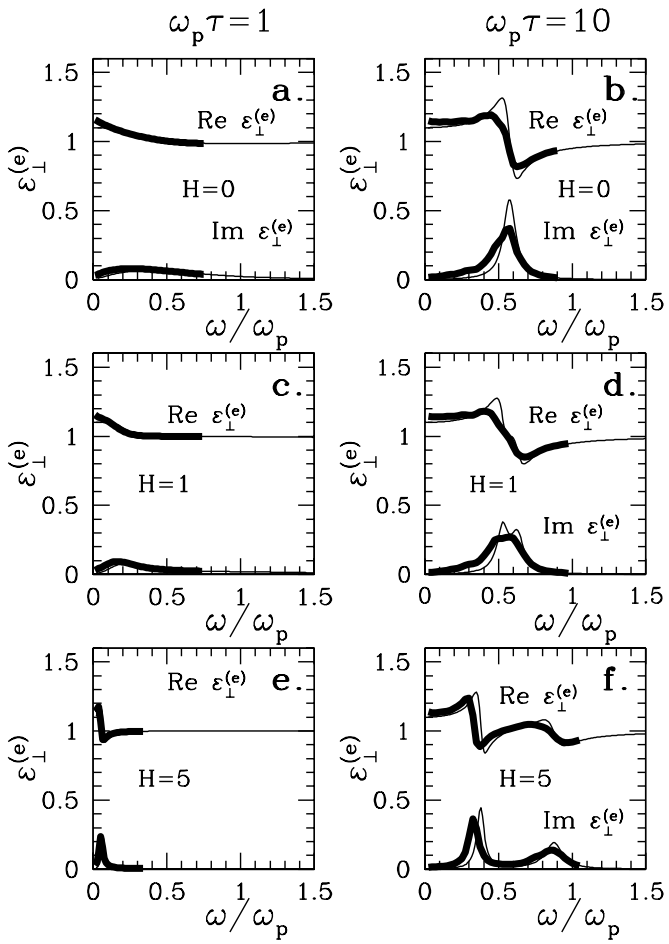

Fig. 1. $\mathrm{Re}(\varepsilon_\perp^{(\mathrm{e})})$ and $\mathrm{Im}(\varepsilon_\perp^{(\mathrm{e})})$ *vs.* frequency ω for the two different values $\omega_\mathrm{p}\tau = 1$ and $\omega_\mathrm{p}\tau = 10$ and for different values of H. Curves shown by thin lines are calculated for the dilute system using equations (11–17), while the curves shown by thick lines are obtained using the numerical method developed in references [1,2]. It is considered the case of composite with spherical inclusions ($\varepsilon_\perp^{(\mathrm{e})} = \varepsilon_{xx}^{(\mathrm{e})} = \varepsilon_{yy}^{(\mathrm{e})}$) for $p_\mathrm{inc} = 0.03$.

2.3 Resonances

The determinant $D(\omega)$ (see Eq. (15)) plays a crucial role when it is equal to zero. In the case of a *spherical* inclusion, this gives a complex quartic equation for the resonance frequency. For $H = 0$ we immediately obtain the frequency $\omega_\mathrm{r} = \omega_\mathrm{p}\sqrt{n_x}$, which is known as a "surface plasmon resonance". However, as soon as $H > 0$, this splits into two resonances: a "magneto-plasma resonance" (denoted by ω_-) and a "magneto-plasma shifted cyclotron resonance" (denoted by ω_+). When the magnetic field is weak so that $\omega_\mathrm{c} \ll \omega_\mathrm{p}$, then for a spherical inclusion ($n_x = 1/3$) these two resonances occur [10–12] at

$$\omega_\pm \cong \omega_\mathrm{p}/\sqrt{3\varepsilon_\mathrm{inc}} \pm \omega_\mathrm{c}/2 + 3\sqrt{3\varepsilon_\mathrm{inc}}\omega_\mathrm{c}^2/(8\omega_\mathrm{p}), \qquad (18)$$

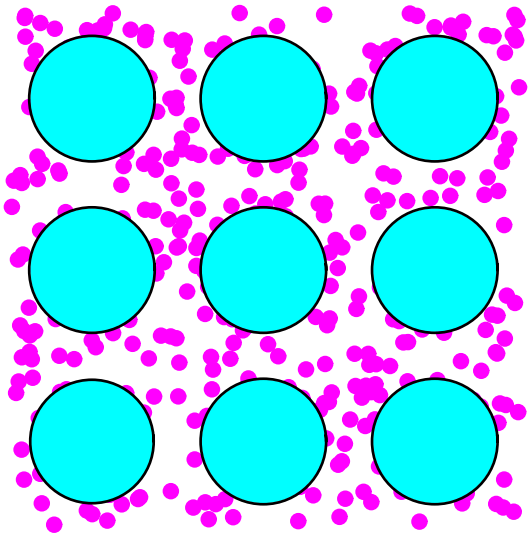

Fig. 2. Idealized picture of a composite where the host is itself a composite medium made of a normal dielectric material with a random distribution of small metallic inclusions. A periodic array of much larger normal dielectric inclusions is embedded inside this composite host.

while when the magnetic field is strong so that $\omega_\mathrm{c} \gg \omega_\mathrm{p}$, they occur at

$$\omega_- \cong \omega_\mathrm{p}^2/(3\varepsilon_\mathrm{inc}\omega_\mathrm{c}), \qquad (19)$$

$$\omega_+ \cong \omega_\mathrm{c} + \omega_p^2/(3\varepsilon_\mathrm{inc}\omega_\mathrm{c}). \qquad (20)$$

In Figure 1 we show this behavior by plotting $\varepsilon_{xx}^{(\mathrm{e})}$ *vs.* ω, using the approximation of (17), and also using numerically calculated values. The latter were calculated using a method developed earlier in the context of DC magneto-transport [2], which is based upon solving a truncated set of linear algebraic equations for the Fourier expansion coefficients of (7).

3 Two length scales

It is known that conducting and dielectric composites are both described [2,7] by equations very similar to equations (1–6), using the position dependent conductivity or permittivity tensors $\hat{\boldsymbol{\sigma}}$, $\hat{\boldsymbol{\varepsilon}}$, respectively. In the AC case the difference between the two descriptions becomes even less significant since both tensors are combined into one complex permittivity tensor (11). Therefore we can expect some similarities between the magneto-transport and magneto-optical properties of composites.

Recent studies of the bulk effective DC conductivity tensor $\hat{\boldsymbol{\sigma}}^{(\mathrm{e})}$ of conducting composites have shown that when the antisymmetric off-diagonal terms of the local conductivity tensor are large, *i.e.*, $|\sigma_{xy}/\sigma_{xx}| \gg 1$ then, in the case of a periodic microstructure, the components of $\hat{\boldsymbol{\sigma}}^{(\mathrm{e})}$ all become strongly dependent on the precise orientation of $\mathbf{B}$ and of the volume averaged current density $\langle \mathbf{J} \rangle$ with respect to the microstructure [1–5].

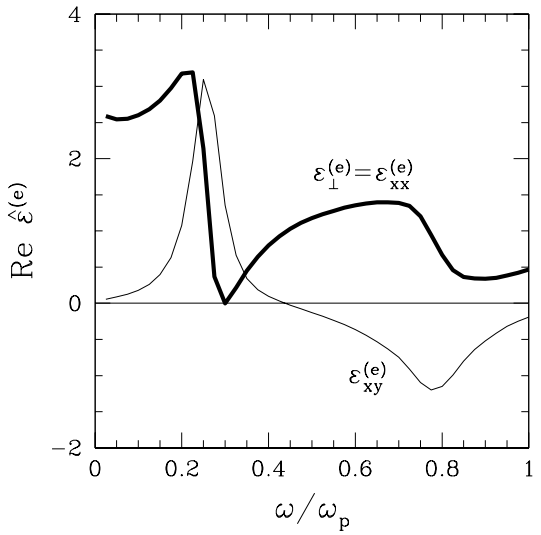

Fig. 3. Dispersion curves of $\mathrm{Re}(\varepsilon_{xx}^{(e)})$ (thick lines) and $\mathrm{Re}(\varepsilon_{xy}^{(e)})$ (thin lines) calculated for the case of spherical inclusions ($p_{\mathrm{inc}} = 0.26$) at $H = 3$ and $\omega_p\tau = 10$. For such values of p_{inc}, $\omega_p\tau$, and H the off-diagonal term $\varepsilon_{xy}^{(e)}$ is larger than 1, while the diagonal term $\varepsilon_{xx}^{(e)}$ takes the near zero value at $\omega \cong 0.3\omega_p$. Therefore, the ratio $\varepsilon_{xy}^{(e)}/\varepsilon_{xx}^{(e)}$ could be extremely large for this case.

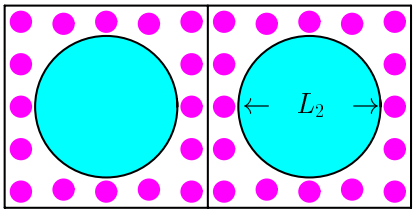

(a)

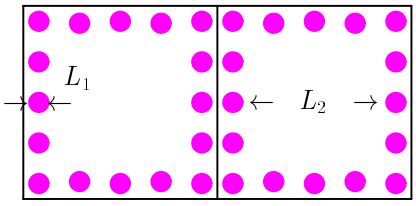

(b)

Fig. 4. Modified picture of the composite shown in Figure 2. The small conducting inclusions of the length L_1 (first characteristic length scale) are placed along the perimeter of the unit cell in order to create an effective composite dielectric host with a large off-diagonal-to-diagonal ratio. Then a conducting (see (a)) or insulating (see (b)) island in the center of the unit cell serves as an effective obstacle (second characteristic length scale).

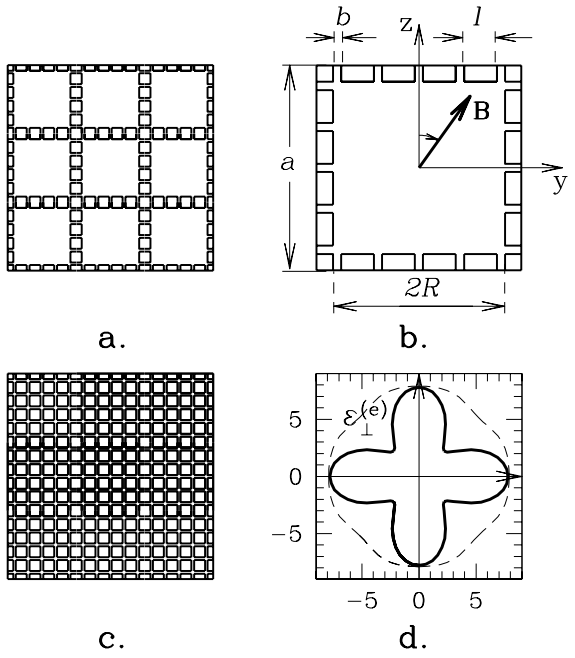

Fig. 5. (a) Schematic drawing of a two-heterogeneity-lengths periodic microstructure made of rows and columns of small, tightly spaced inclusions. (b) A square unit cell of the periodic microstructure used in our calculations: the small squares represent a cross-section of the infinitely long metal rods that lie parallel to the x axis. The size parameters were $l/a = 0.16$, $b/a = 0.04$, $R/a = 0.4$. The two important size scales in this system are represented, we believe, by b and $2R$, which differ by a factor 20. (c) It is shown how the pure composite host would look like. (d) Polar plot of the bulk effective transverse electric permittivity $\varepsilon_{\perp}^{(e)}$ of the periodic composite with the unit cell shown in (b) — solid line shows the real part, dashed line the imaginary part. The magnetic field **B** has a fixed magnitude and is rotated in the film y, z plane. The angular frequency of the applied electric field is $\omega = 0.3\omega_p$, and lies in the resonance region, where the off-diagonal-to-diagonal ratio would be large if the composite looks like is shown in (c). The dielectric constant of the host was taken to be $\varepsilon = 10$, while the electric permittivity tensor of the inclusions was taken to have the form of equations (11–12) with $\varepsilon_{\mathrm{inc}} = 10$, $\omega_c\tau = \mu|\mathbf{B}| = H = 5$ and $\omega_p\tau = 35$.

Because the magneto-electric behavior of a metal-dielectric composite in the quasi-static regime depends upon the microstructure in the same way as the DC magneto-transport behavior described above, we expect that similar effects will be observed, when the permittivity of the dielectric host material has a large antisymmetric part. Since it is not easy to find such a naturally occurring dielectric material, we therefore explored the possibility of using a composite metal-dielectric medium as a non-standard dielectric host, where ε_{xy} can be nonzero due to the presence of a Hall conductivity component in the complex AC permittivity. In this non-standard host we can embed a periodic array of much larger inclusions which would again be made of a standard dielectric material — see Figure 2.

When we considered a non-dilute composite and **B** is not too small, we first found (numerically, as well as analytically using a Clausius-Mossotti-type approximation [10]) that the frequency of the magneto-plasma resonance depends not only on the shape (*i.e.*, depolarization factor) but also on the size of the inclusions (*i.e.*, on the volume fraction p_{inc}). Moreover, we found

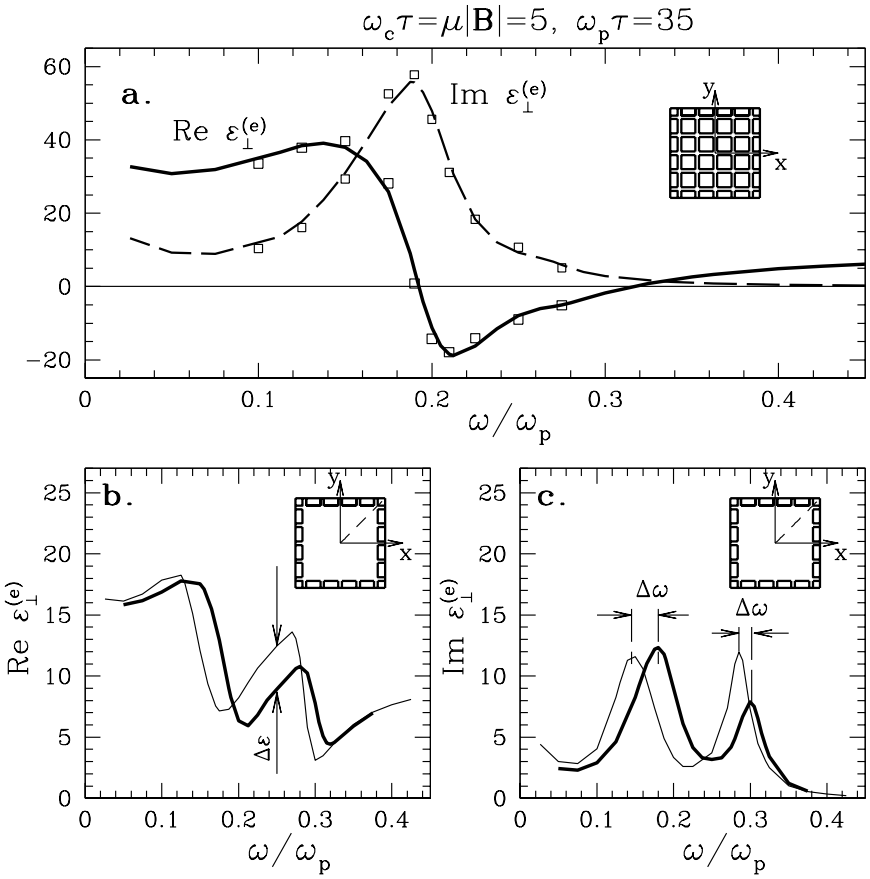

Fig. 6. (a) $\mathrm{Re}(\varepsilon_\perp^{(\mathrm{e})})$ and $\mathrm{Im}(\varepsilon_\perp^{(\mathrm{e})})$ *vs.* frequency ω for the "simple" composite medium of Figure 5c (see inset), made of a square array of parallel metallic rods with square cross-section embedded in a dielectric host. The externally applied magnetic field $\mathbf{B}$ corresponds to $\omega_\mathrm{c}\tau = \mu\mathbf{B} = 5$ in the inclusions, and the zero field plasma frequency corresponds to $\omega_\mathrm{p}\tau = 35$. The lines show the frequency dependence of $\varepsilon_\perp^{(\mathrm{e})}$ when $\mathbf{B} \parallel (100)$, while the empty squares show that dependence when $\mathbf{B} \parallel (110)$. (b) and (c) Same as (a), but for the composite medium of Figure 5a (see inset) with two different microstructural length scales. Note that the single resonance of (a) splits into two resonances, and that the exact positions of those resonances depend on the direction of $\mathbf{B}$. The thick solid lines correspond to $\mathbf{B} \parallel (100)$, while the thin solid lines correspond to $\mathbf{B} \parallel (110)$.

that the diagonal component $\varepsilon_{xx}^{(\mathrm{e})}$ and the anti-symmetric off-diagonal component $\varepsilon_{xy}^{(\mathrm{e})}$ go through 0 at *different frequencies* — see Figure 3 and reference [10]. Thus, we can achieve a composite medium with a large ratio $\varepsilon_{xy}/\varepsilon_{xx}$ (since $\varepsilon_{xx} \to 0$ while $\varepsilon_{xy} \neq 0$) in the vicinity of any sharp quasi-static resonance.

Motivated by this observation we expected that it would be possible to obtain the required anisotropy even in a simpler microstructure than the one shown in Figure 2. The idea was to place all the inclusions in a periodic array but with *two different characteristic length scales*, as shown in Figure 4. The unit cell of the composite microstructure which we used in our calculations is shown in Figure 5b. It is made by arranging a sequence of square-cross-section rods (first characteristic length scale) along the perimeter of a square unit cell, in order to create an effective composite dielectric host with a large off-diagonal-to-diagonal permittivity ratio. The dielectric (of size $2R$ — see Fig. 5b) at the center of the unit cell then plays the role of a large dielectric inclusion (second characteristic length scale). However, by changing from a spherical to cylindrical geometry there appears an uncertainty: it is not clear which of the ratios $\varepsilon_{xy}/\varepsilon_{xx}$ or $\varepsilon_{yx}/\varepsilon_{yy}$ plays a role analogous to that of $H = \sigma_{xy}/\sigma_{xx}$ in the DC case [1, 2]. In the case of spherical inclusions this does not matter since $\varepsilon_{xx} = \varepsilon_{yy}$, but in the case of cylindrical inclusions it can be important since now $\varepsilon_{xx} \neq \varepsilon_{yy}$. In spite of the fact that the detailed theory [13] of this AC phenomenon is not complete, the numerical calculations show a well-developed angular anisotropy for samples with two length scales, which is completely absent in samples with only one length scale — see Figure 6. An angular dependence of $\hat{\boldsymbol{\varepsilon}}^{(\mathrm{e})}$ on the direction of the applied static magnetic field $\mathbf{B}$ is observed when the frequency is in the vicinity of one of the sharp resonances, but is absent at frequencies far away from the resonance region. Anisotropy of this kind cannot appear in the simple low density or Clausius-Mossotti-type approximations described above, which ignore all details of the microstructure, in particular its periodic nature. In order to look for such behavior in magneto-optical properties, for which the periodic arrangement of the inclusions is important, we had to use the numerical method

of references [1,2], which is valid for arbitrary volume fraction of the inclusions. In Figure 5d we show a polar plot of the real and imaginary parts of the transverse diagonal component of $\hat{\boldsymbol{\varepsilon}}^{(\mathrm{e})}$, for the case where both $\mathbf{B}$ and $\langle\mathbf{E}\rangle$ are in the film plane and remain perpendicular to each other as $\mathbf{B}$ is rotated in that plane (see Fig. 5b). A similar, well-developed anisotropy is also obtained for the Faraday ϕ_{F} and Kerr ϕ_{K} rotations, as well as for the related ellipticities e_{F}, e_{K}.

4 Conclusion

The parameter values used in our calculation can be realized in an experiment: for example, by using intrinsic InAs as the dielectric host, with $\varepsilon = 10$, and Si-doped InAs rods as the metal inclusions, with $\varepsilon_{\mathrm{inc}} = 10$, a negative charge carrier density $n = 6 \times 10^{16}$ cm^{-3}, an effective mass $m = 0.023\, m_{\mathrm{e}}$ (m_{e} is the bare mass of a free electron), and a Hall mobility $\mu = 3$ m^2(V s)$^{-1}$ (note that $\omega_{\mathrm{c}}\tau = \mu|\mathbf{B}|$, and that this is equal to the Hall-to-Ohmic resistivity ratio). These translate into a bulk plasma frequency $\omega_{\mathrm{p}} \cong 0.9 \times 10^{14}$ s^{-1}, an Ohmic conductivity $\sigma \cong 280$ $(\Omega\,\mathrm{cm})^{-1}$, a relaxation time $\tau \cong 4 \times 10^{-13}$ s, and a mean free path $\ell \cong 220$ nm. With these values, the assumed value of $\omega_{\mathrm{c}}\tau = 5$ can be obtained by using a magnetic field of 1.7 tesla, and an angular frequency of the electric field of about 2.7×10^{13} s^{-1}, thus $\omega\tau \cong 10$. This translates into a wavelength in vacuum of $\lambda_0 \cong 70$ μm, a wavelength inside the semiconductor of $\lambda_{\mathrm{s}} \cong 22$ μm, and a skin depth $\delta \cong 1.5$ μm. These are all large compared to the mean free path ℓ and to the typical de Broglie wavelength $\lambda_{\mathrm{e}} \cong 50$ nm of the charge carriers. This is necessary in order that our complete neglect of ballistic effects and quantum properties of the charge carriers be a good approximation [5]. To this end, it is also necessary that the system be held at a temperature T that is not too low, namely $k_{\mathrm{B}}T > \hbar\omega_{\mathrm{c}}$, which means $T > 90$ K. It is also necessary that the length scales which characterize the relevant aspects of the microstructure lie in between the two physical length scales mentioned above. This means that the length parameters l, a, and $2R$ of Figure 5b must satisfy

$$\ell, \lambda_{\mathrm{e}} \ll l, a, 2R \ll \lambda_{\mathrm{s}}, \delta. \tag{21}$$

Finally, we hope that the results presented here will stimulate experimental studies aimed at verification of our predictions and continued exploration of the magneto-optical properties of such systems.

This research was supported in part by grants from the US-Israel Binational Science Foundation, the Israel Science Foundation, the Tel Aviv University Research Authority, and the Gileady Fellowship program of the Ministry of Absorption of the State of Israel.

References

1. D.J. Bergman, Y.M. Strelniker, Phys. Rev. B **49**, 16256 (1994).
2. Y.M. Strelniker, D.J. Bergman, Phys. Rev. B **50**, 14001 (1994).
3. D.J. Bergman, Y.M. Strelniker, Phys. Rev. B **51**, 13845 (1995).
4. Y.M. Strelniker, D.J. Bergman, Phys. Rev. B **53**, 11051 (1996).
5. M. Tornow, D. Weiss, K. von Klitzing, K. Eberl, D.J. Bergman, Y.M. Strelniker, Phys. Rev. Lett. **77**, 147 (1996).
6. Y.M. Strelniker, D.J. Bergman, Phys. Rev. B **59**, R12763 (1999).
7. P.M. Hui, D. Stroud, Appl. Phys. Lett. **50**, 950 (1987).
8. L.D. Landau, E.M. Lifshitz, L.P. Pitaevskiĭ, *Electrodynamics of Continuous Media*, 2nd edn. (Pergamon Press, New York, 1984).
9. D. Stroud, F.P. Pan, Phys. Rev. B **13**, 1434 (1976).
10. D.J. Bergman, Y.M. Strelniker, Phys. Rev. Lett. **80**, 857 (1998).
11. G. Dresselhaus, A.F. Kip, C. Kittel, Phys. Rev. **100**, 618 (1955).
12. G. Dresselhaus, A.F. Kip, C. Kittel, Phys. Rev. **98**, 369 (1955).
13. D.J. Bergman, Y.M. Strelniker (unpublished).